Chapter 4

SYNERGISTIC ORDERING OF SIDE-GROUP LIQUID CRYSTAL POLYMER AND SMALL MOLECULE LIQUID CRYSTAL: ORDER AND PHASE BEHAVIOR OF NEMATIC POLYMER SOLUTIONS

4.1 Introduction

4.1.1 Background

Random-coil polymers are rarely soluble in small-molecule nematic liquid crystals (LCs) because the solvent's orientational order presents a large entropic penalty to dissolution.[1, 2] Decorating the polymer backbone with liquid crystalline moieties yields a side-group liquid crystal polymer (SGLCP) with orientational order of its own. Nematic interactions with the polymer side-groups make it possible to dissolve an SGLCP in an LC solvent, and rich

phase behavior results from the thermodynamic balance between liquid crystalline order and the consequently anisotropic conformation of the polymer backbone. [3-16]

Mixtures of SGLCPs and small-molecule LCs usually have a transition to the isotropic phase that occurs at temperatures near or below the isotropization temperatures of the pure components;[3-14] in rare instances the mixture's isotropization point may lie slightly above that of the pure components.[16]   Mixtures of SGLCP and LC also often exhibit isotropic-nematic or nematic-nematic coexistence between fully nematic and fully isotropic states.[3, 4, 7-14, 16]   Phase diagrams similar to observed behavior (and a host of others yet to be observed) can be derived from Brochard's mean-field theory[12, 15] combining the Flory-Huggins theory of mixing with the Maier-Saupe theory for nematic order. Within the Brochard model, the nematic order parameters predicted by the Maier-Saupe theory strongly influence the free energy of an SGLCP/LC mixture; however, there have been surprisingly few studies in which the component order parameters were measured in conjunction with the mixture's phase behavior. The few that exist examine main-chain liquid crystal polymers,[17, 18] for which Brochard's theory breaks down because of the strong coupling of liquid crystalline order to polymer conformation.

Here we examine the phase behavior and the order parameter of each component in an SGLCP/LC mixture. Calorimetry shows that nematic order can be strongly stabilized in the mixtures relative to the pure components: there exist compositions that have isotropization points more than 15 °C greater than that of either component and have latent heats of transition much greater than either pure component. This cooperative ordering at high polymer concentration (~80 wt %) occurs despite the opposite tendency at low polymer concentration, leading to strikingly non-monotonic effects of concentration. The underlying molecular order of each component in the solutions is characterized using deuterium labeling and ^{2}H NMR spectroscopy; the solutions' overall order parameters are assessed using birefringence measurements. The results demonstrate a strong coupling between liquid crystalline order and polymer conformational entropy that is unique in comparison to the prior literature on mixtures of SGLCPs with small-molecule nematic LCs.

4.1.2 Theory

Brochard's model for predicting the phase behavior of SGLCPs and small-molecule LCs assumes complete decoupling between the polymer backbone and the orientational order of the attached mesogens. The molar free energy, G, is calculated from the sum of an isotropic contribution, G_{iso}, and a nematic contribution, G_{nem}. The isotropic free energy is given by the Flory-Huggins theory for dissolving a polymer, B, with degree of polymerization N_B in a small-molecule solvent, A:

$$G_{iso} = kT\left[\phi_A \ln \phi_A + \frac{(1-\phi_A)}{N_B}\ln(1-\phi_A) + \chi\phi_A(1-\phi_A)\right],$$ (4.1)

where χ is the Flory interaction parameter, ϕ_A is the volume fraction of species A, T is the temperature and k is Boltzmann's constant. The nematic free energy is given by the Maier-Saupe model:

$$G_{nem} = -\tfrac{1}{2}U_{AA}S_A^2\phi_A^2 - \tfrac{1}{2}U_{BB}S_B^2(1-\phi_A)^2 - U_{AB}S_A S_B\phi_A(1-\phi_A) - T\Sigma(S_A)\phi_A - T\Sigma(S_B)(1-\phi_A),$$
(4.2)

where S_A and S_B are the nematic order parameters of the solvent and polymer, respectively, and U_{AA}, U_{BB}, and U_{AB} are the pairwise nematic interaction parameters of two solvent mesogens, two polymer mesogens, and a solvent mesogen with a polymer mesogen, respectively. These nematic interactions are assumed to arise from van der Waals interactions between the molecules. The final two terms express the loss of entropy due to LC order that is described below.

The order parameters in G_{nem} are functions of temperature, composition, and the nematic interaction parameters and are evaluated numerically as a function of temperature and composition. Brochard uses the usual approximation of U_{ij} independent of temperature and the familiar relationship between the pure-component isotropization temperature, T_A or T_B, and its self-interaction:

$$\frac{kT_A}{U_{AA}} = \frac{kT_B}{U_{BB}} = \frac{1}{\alpha_c}, \quad \alpha_c = 4.54.^{[19]}$$ (4.3)

The cross interaction parameter, U_{AB}, is assumed to be related to U_{AA} and U_{BB} by

$$U_{AB} = c\sqrt{U_{AA}U_{BB}},$$ (4.4)

where c is an unknown proportionality constant.[12, 13] If $c < 1$, nematic interactions between the polymer and solvent are unfavorable and the nematic phase is destabilized by mixing. If $c > 1$, nematic interactions between the polymer and solvent are stronger than in either pure component. At fixed T and ϕ_A, the individual species adopt individual order parameters that minimize the free energy of nematic interactions, completely decoupled from the conformational entropy of the polymer. The penalty for deviation of the orientation of species i from the director is coupled to that of the other species. The severity of the penalty for misalignment is captured by the field parameters, m_i, of the Maier-Saupe theory adapted for mixtures:

$$m_A = \frac{\frac{3}{2}U_{AA}}{kT}S_A\phi_A + \frac{\frac{3}{2}U_{AB}}{kT}S_B(1-\phi_A)$$

$$m_B = \frac{\frac{3}{2}U_{BB}}{kT}S_B(1-\phi_A) + \frac{\frac{3}{2}U_{AB}}{kT}S_A\phi_A$$

[12, 15, 19]

(4.5)

The greater m_i, the sharper the orientation distribution of species i ($m_i \rightarrow \infty$ gives a δ-function and $m_i \rightarrow 0$ gives a perfectly isotropic distribution). Therefore, the S_i's in Equation 4.5 must simultaneously satisfy

$$S_i = -\frac{1}{2} + \frac{3}{2Z_i}\int_0^1 x^2 \exp(m_i x^2)dx,$$

(4.6)

where the partition function, Z_i, is given by

$$Z_i = \int_0^1 \exp(m_i x^2)dx.$$

(4.7)

At fixed values of T and ϕ_A, S_A is solved as a function of S_B, and vice versa, and the intersection of the two curves gives the solution.

With the order parameters known, G_{nem} is calculated from Equation 4.2 with the entropy terms given by

$$\Sigma(S_i) = -k\left(\log\frac{4\pi}{Z_i} + m_i S_i\right).[15]$$

(4.8)

When both order parameters fall below the critical value of $S_i = 0.429$ the nematic phase is unstable and G_{nem} is set to zero. The total free energy is calculated from $G = G_{nem} + G_{iso}$ assuming the Flory interaction parameter is proportional to the reciprocal of temperature

($\chi = A / T$) and two-phase coexistence is indicated when a single tangent line connects two points on $G(\phi_A)$ curve with fixed T.[12, 15]

4.2 Experimental

4.2.1 Materials

Two side-group liquid crystal homopolymers, 350HSiCB4 and 490HSiCB4, were synthesized according to the methods described in Appendix A. Isotopic labeling of the side-group was performed according to the method described in Appendix B and the labeled side-group was used to synthesize $d_2$350HSiCB4, the deuterium-labeled analog of 350HSiCB4 (Figure 4.1). These polymers' properties are summarized in Table 4.1 and the details of their characterization may be found in Appendix A.

Solutions of these polymers in the nematic LC 4-pentyl-4′-cyanobiphenyl (5CB, used as received from TCI America) were prepared by dissolving the two together in dichloromethane (DCM) then evaporating the DCM under a stream of air followed by drying in vacuum overnight.

4.2.2 Differential Scanning Calorimetry (DSC)

Differential scanning calorimetry (DSC) was performed using a Perkin-Elmer DSC 7 calorimeter. Each sample consisted of between 10 and 20 mg of solution contained in an aluminum pan and loosely covered with an aluminum lid. The pans were not sealed so as to avoid squeezing the solution out during the crimping process. Prior to loading a sample, the calorimeter's empty sample chamber was heated to 200 °C for a few minutes to drive off any residual moisture then cooled to 20 °C. Temperature scans were performed at a rate of 10 °C/min in a maximum range of 20 to 100 °C; the actual range used for a given sample was chosen to encompass the nematic-isotropic transition. The data from at least the first three full cycles of heating and cooling were discarded: data were retained when six consecutive cycles gave virtually indistinguishable results.

The onset temperature and latent heat of the nematic-isotropic phase transition were calculated from DSC data using Perkin-Elmer's Pyris® software (version 3.04). Since the heat flow versus time data has a sloping baseline, the data was numerically differentiated and ranges where the second derivative was non-zero were used to select the beginning and end points for integration. The results from six separate scans were averaged to arrive at the onset temperatures of the phase transitions on heating and on cooling. Random errors in the data sets are primarily associated with choosing the limits of integration.

A baseline subtraction and normalization procedure was applied to DSC temperature scans to aid in visualizing qualitative differences in the nematic-isotropic transition endotherms. The magnitude and the temperature-dependence of the heat capacity differs between the nematic and isotropic phase. Therefore, a quadratic fit of the baseline was performed in regions well below and well above the phase transition. To estimate a baseline underlying the phase transition itself, the two fits were extrapolated inside the transition and spliced together at the temperature that minimized the difference between the two polynomials (they would ideally be equal). The piecewise fit was subtracted from the data, which was then divided by the sample mass to give the normalized, subtracted heat flow, Q, due to the phase transition. Note that the discontinuity in the spliced baseline gives rise to a discontinuity in $Q(T)$.

4.2.3 Polarized Optical Microscopy (POM)

Polarized optical microscopy (POM) was performed using a Zeiss Universal stereomicroscope with temperature controlled by a Mettler FP82 hot stage. A small amount of polymer was placed on a microscope slide and the colorful, birefringent texture was observed between crossed polarizers while the temperature was ramped at a rate of 10 °C/min.

4.2.4 Deuterium Nuclear Magnetic Resonance Spectroscopy (^{2}H NMR)

Deuterium NMR spectra were recorded at a variety of temperatures using a Bruker Avance 200 MHz solid-state NMR spectrometer tuned to 30.73 MHz. Approximately 250 mg of polymer solution was loaded into a zirconium NMR rotor 7 mm in diameter and cooled

from the isotropic phase inside the magnet to ensure alignment of the LC director parallel to the magnetic field. The sample was equilibrated at the desired temperature for 15 minutes prior to beginning data acquisition. Spectra were acquired statically using a solid-echo pulse sequence with proton decoupling and averaging between 32 and 512 scans, depending on the signal strength.

The NMR spectrometer's thermocouple was brought into registration with that of the microscope hot stage and the DSC using the liquid crystal itself: the transition temperature (T_{NI}) of each sample determined by POM (the temperature at which a sample's colored, birefringent texture disappeared) or from DSC (onset temperature upon heating) was compared to the temperature at which a single peak characteristic of an isotropic sample was first observed by ^{2}H NMR. The spectrometer's temperature controller only permits control to the nearest degree. For the purposes of these experiments, the T_{NI} was taken as the first temperature at which an isotropic ^{2}H NMR spectrum was recorded when successively increasing temperature in increments of 1 °C. The thermocouple of the spectrometer was systematically 3 °C below that of the hot stage or the DSC.

Deuterium was incorporated into the SGLCP ($d_2$350HSiCB4) or into the LC solvent by mixing d_{19}5CB with 5CB. Since the T_{NI} of d_{19}5CB (~32 °C) is substantially lower than that of 5CB (35 °C) its concentration was kept below 5 wt % in order to keep each sample's transition temperature within 1 °C of an equivalent hydrogenous sample.

4.2.5 Refractive Index Measurement

The ordinary and extraordinary refractive indices (n_o and n_e) of mixtures of 490HSiCB4 and 5CB were measured in an Atago 4T Abbe refractometer illuminated by LEDs having a peak wavelength of 630 nm and with temperature control of ± 0.1 °C achieved using circulated water from a Fisher Scientific Isotemp Refrigerated Circulator Model 900. The refractometer was calibrated with liquid standards to read the index of refraction for light with 633 nm wavelength. Monodomain samples having a uniformly aligned LC director are required to measure both n_o and n_e.[20] Alignment was achieved by coating the prisms of the refractometer with a solution of 1 % lecithin in chloroform. When the lecithin

alignment layer alone was inadequate, monodomain alignment was achieved by wiggling the top prism to create shear stresses large enough to induce some macroscopic order. Prior literature on a similar polymer[21] dissolved in 5CB at similar concentration showed that shear causes the director to align near the velocity gradient direction, here normal to the prism surfaces. The birefringence of an LC monodomain causes light with different polarizations to refract at different angles; instead of the single line separating a light and dark area observed in isotropic fluids, a polarizer is used to visualize the two indices. In one orientation, a change from a bright to a dimmer region is seen at n_e and when rotated 90° a second line corresponding to n_o is observed.

4.3 Results

4.3.1 Differential Scanning Calorimetry (DSC)

All mixtures of 350HSiCB4 and 5CB with polymer concentrations ranging from 0 to 100 wt % are nematic at room temperature and undergo a transition to the isotropic phase, indicated by an endothermic peak in the DSC trace, somewhere in the temperature range of 30 to 90 °C. The onset temperature of the transition shows a strikingly non-monotonic dependence on polymer concentration: at low polymer concentration (0 to 20 wt %) the position of the peak changes very little with concentration, it shifts to higher T in the range of 20 to 78 wt %, and shifts to lower T as concentration is further increased. In two ranges of polymer concentration, approximately 20 to 70 wt % and 85 to 95 wt %, the nematic to isotropic phase transition takes place over a broad temperature range and a shoulder is often observed in the phase transition endotherm (Figure 4.3). Although POM shows no evidence of two-phase coexistence in either the nematic or isotropic phase, the broad transitions are attributed to a biphasic region near the phase transition. We suspect that two-phase coexistence is difficult to detect by POM because the coarsening of phase separation to observable length scales is very slow, particularly for polymer concentrations of 20 wt % or more.

The qualitative trends observed in the DSC traces are reflected in the concentration dependence of the nematic to isotropic phase transition's onset temperature, T, and latent

heat, $|\Delta H|$ (Figure 4.4). At concentrations less than 20 wt % polymer the onset temperature during heating is relatively constant, but in the range of 20 to 78 wt % polymer it increases sharply (Figure 4.4a), eclipsing the onset temperature of either of the pure components by a wide margin (it reaches a maximum of 80.5 °C, much greater than 36.2 °C and 63.0 °C for pure 5CB and bulk polymer, respectively). The onset temperature decreases with further increase in concentration beyond 80 wt %, and the transition becomes remarkably broad. The peculiarly broad transition observed at 91 wt % polymer (spanning > 20 °C range) is not inherent to the polymer itself, which has a single peak with a full width at half-maximum less than 3 °C. Small differences between the onset temperatures on heating versus cooling are attributed to the subcooling regularly observed in LC phase transitions. Corresponding features are evident in the transition enthalpies (Figure 4.4b). The measured value of $|\Delta H|$ on heating for pure 5CB is 2.01 ± 0.07 J/g, in good agreement with values reported in the literature[22, 23] (2.00 J/g or 1.56 J/g). For the bulk polymer $|\Delta H|$ on heating is 4.23 ± 0.03 J/g, which is much greater than values reported for other SGLCPs (0.53 and 1.9 J/g).[5, 24] In the range of 0 to 20 wt % polymer, $|\Delta H|$ decreases slightly with increasing concentration. Above 20 wt % the latent heat increases sharply with concentration, reaching a maximum (6.34 ± 0.05 J/g) at 83 wt % polymer that is substantially greater than either pure component. Between 83 and 91 wt %, $|\Delta H|$ again decreases with concentration. The concentration-dependence of $|\Delta H|$ is in stark contrast to the linear dependence reported by Finkelmann, Kock, and Rehage.[5]

4.3.2 Deuterium Nuclear Magnetic Resonance Spectroscopy (^{2}H NMR)

^{2}H NMR spectra were collected from samples containing between 0 and 10 wt % SGLCP with deuterium incorporated into either the solvent or the polymer's side groups. In the nematic phase, the spectra from d_{19}5CB consist of pairs of peaks symmetric about a frequency, ν, of 0 kHz with splittings, $\Delta\nu$, that depend on temperature (Figure 4.5a). The spectra from $d_2$35OHSiCB4 consist of one pair of symmetric peaks centered about $\nu = 0$ kHz, also split by a temperature-dependent magnitude, $\Delta\nu$. The splitting derives from the deuterons' quadrupolar interactions with the local electric field gradient and when the director is parallel to the magnetic field, as is the case in these experiments, its magnitude is

directly proportional to the microscopic order parameter, S_{ZZ}, of the C-D bond of interest:[25]

$$\Delta \nu = \tfrac{3}{2} Q_{CD}^{Ar} \frac{3\cos^2\theta - 1}{2} S_{ZZ}, \tag{4.9}$$

Where S_{zz} accounts for the orientation distribution of the molecule's long axis, $\boldsymbol{u}$, with respect to the magnetic field, $\boldsymbol{H}$, ½ (3 $\cos^2 \theta$ -1) accounts for the orientation angle of the C-D bond with respect to the molecular axis, $\boldsymbol{u}$, and Q_{CD}^{Ar} is the quadrupolar coupling constant equal to 185 kHz for aromatic deuterons.[26] For the purposes of making comparisons between the orientational order of the solvent and the polymer side groups, the measurement of $\Delta \nu$ from d$_{19}$5CB is restricted to deuterons located *para-* to the alkyl chain (site "d" in Figure 4.5) since they are geometrically equivalent to the deuterons of d$_2$350HSiCB4. Emsley, Luckhurst, and Stockley have found θ = 60.6° for these deuterons in d$_{19}$5CB,[27] and previous measurements of the quadrupolar splittings of 4-hexyloxy-4′-cyanobiphenyl (6OCB) have demonstrated that the geometry of the aromatic deuterons located *para-* to the oxygen atom is not significantly different.[26, 28] When the polymer concentration exceeds 10 wt % the peaks in the nematic phase become broad and difficult to distinguish, possibly due to poor alignment of the LC molecules with the magnetic field.

In the isotropic phase the spectra from both d$_{19}$5CB and d$_2$350HSiCB4 consist of a single peak centered at ν = 0 kHz (Figure 4.5b). At temperatures 1 or 2 °C below the nominal T_{NI}, ^{2}H NMR spectra from d$_{19}$5CB and d$_2$350HSiCB4 have both an isotropic peak at ν = 0 kHz and nematic peaks split by $\Delta \nu$. The presence of both nematic and isotropic character in the spectra near T_{NI} is attributed to pretransitional orientation fluctuations induced by the strong magnetic field,[29] and should not be taken as a sign of two-phase nematic/isotropic coexistence.

The measured values of $\Delta \nu$ for the distinguishable deuterons in d$_{19}$5CB in the absence of polymer are within 5% of those reported by Auger et al.[30] All of these splittings decrease when polymer is added. Thus, the order parameter of the LC solvent decreases when polymer is dissolved in it (inset in Figure 4.6a). At each concentration, the order parameter of the polymer is consistently lower than that of the LC solvent (Figure 4.6): for example,

at 5 wt % polymer and $T = T_{NI}$ - 9 °C, S_{ZZ}^{5CB} = 0.31 and $S_{ZZ}^{350HSiCB4}$ = 0.25. As the concentration of polymer increases, S_{ZZ} of $d_{19}5CB$ decreases (Figure 4.6a). On the other hand, S_{ZZ} of $d_2350HSiCB4$ is relatively insensitive to polymer concentration (Figure 4.6b).

4.3.3 Refractive Indices

The temperature-dependent ordinary and extraordinary refractive indices (n_o and n_e, respectively) measured for pure 5CB (Figure 4.7) are within 0.5% of the values reported by Karat and Madhusudana.[31] The effect of polymer on both n_o and n_e could be measured up to 10 wt %; however, n_e could not be measured for 20 wt % 490HSiCB4 because the sample alignment was poor and at concentrations > 20 wt %, neither n_o nor n_e could be measured accurately. Addition of polymer distinctly reduces n_e, over the range of accessible concentrations. The ordinary refractive index is relatively insensitive to polymer concentration, showing a slight increase with increasing concentration. The refractive index in the isotropic phase, n_{iso} is also insensitive to added polymer, showing a slight decrease with addition of polymer.

The nematic order parameter, S, is calculated from the ordinary and extraordinary refractive indices using the method described by Haller et al.[32] The order parameter is related to n_o and n_e by

$$S = \frac{n_e^2 - n_o^2}{n_{avg}^2 - 1} \frac{\langle \alpha \rangle}{\Delta \alpha},$$

(4.10)

where $n_{avg}^2 = \frac{1}{3}n_e^2 + \frac{2}{3}n_o^2$, $\Delta\alpha$ is the anisotropy of the polarizability, and $\langle \alpha \rangle$ is the average polarizability.[31-33] The Haller analysis aims to estimate the ratio $\langle \alpha \rangle / \Delta \alpha$ from the temperature dependence of n_o and n_e, using the empirical observation that log[$S\Delta\alpha$] is proportional to log[$(T_{NI}$ - $T)/T_{NI}$]. The average polarizability is related to the refractive indices by

$$\frac{4\pi\rho N_A}{M}\langle \alpha \rangle = \frac{n_e^2 + 2n_o^2 - 3}{3n_{avg}^2 + 6},$$

(4.11)

where ρ and M are the LC's density and the molar mass, respectively, and N_A is Avogadro's number.[32] Combining Equations 4.10 and 4.11 gives $S\Delta\alpha$ in terms of the

known quantities n_o, n_e, ρ, and M. Plotting $\log[S\Delta\alpha]$ versus $\log[(T_{NI} - T)/T_{NI}]$ and extrapolating to $T = 0$ K, where $S = 1$, gives $\Delta\alpha$. Combined with $<\alpha>$ calculated from Equation 4.11, the order parameter is calculated from the estimate of $<\alpha>/\Delta\alpha$ (Figure 4.8).

The calculated order parameters for 5CB are less than 13% different from those estimated by Karat and Madhusudana.[31] The order parameter of 1 wt % 490HSiCB4 is unchanged from that of 5CB throughout the entire temperature range studied. As polymer concentration is increased to 5 or 10 wt %, the order parameter curve is shifted to progressively lower values (Figure 4.8).

4.4 Discussion

Although we do not have sufficient information to produce the phase diagram of 350HSiCB4 and 5CB, we can deduce its character from the calorimetry results on heating (Figure 4.9a). In particular, the narrow single peak in the endotherm of 78 wt % 350HSiCB4 solution indicates that the phase diagram has a direct transition from the nematic to isotropic phase at that composition, with T_{NI} of approximately 80 °C. At concentrations immediately above and below 78 wt %, two-phase coexistence is indicated by broad endotherms. The biphasic temperature range can be estimated from the measured onset temperature and the temperature at which the transformation to the isotropic phase is complete (the endotherm's intensity final decrease). The DSC traces from solutions with high polymer concentration indicate wide biphasic regions; for example, in 91 wt % 350HSiCB4 the biphasic region may be as wide as 25 °C. On the solvent-rich side, the biphasic region, if it exists, appears to be less than 10 °C wide. Our data do not allow for identification of the coexisting phases (e.g. N + N or N + I).

The Brochard model commonly used to describe the phase behavior of SGLCPs with small molecule LCs can capture some of the characteristics of the 350HSiCB4/5CB phase diagram; however it does not accord with the underlying molecular order. A phase diagram calculated by Chiu and Kyu[12] using the theory for an SGLCP/LC mixture with strong interactions between the different polymer and solvent mesogens $(c = U_{AB}/(U_{AA}U_{BB})^{1/2} = 1.2)$ is somewhat similar to the phase diagram inferred from the

DSC data (Figure 4.9b). The model captures the presence of a stabilized, single nematic phase that transitions to a single isotropic phase at a high temperature relative to the pure components. It also has biphasic windows at compositions above and below the composition having the maximum clearing point. However, owing to the Flory-Huggins treatment of the polymer-solvent interaction in Brochard's model, the theoretical phase diagram predicts the biphasic window to be wider on the solvent-rich side of the phase diagram ($\phi < 0.5$). In contrast, the behavior of 350HSiCB4/5CB suggests a wider biphasic window in polymer-rich solutions. Furthermore, the temperature at which the solution becomes completely isotropic in the model has a concentration dependence that is strictly concave down, whereas the observed isotropization transition changes from concave up to concave down as concentration is increased.

Brochard's theory has been used to model the experimental phase diagrams of SGLCP/LC mixtures,[11-13] and its apparent success cited as evidence that conformational entropy and LC order are decoupled. However, there appears to be no prior verification that the component order parameters are adequately modeled, so it is not known whether the theory's assumptions are substantiated or whether its agreement with observed phase behavior is coincidental. The Brochard model is founded on the Maier-Saupe theory for nematic interactions. Flory-Huggins interactions are included, which can add biphasic windows to the phase diagram, but cannot change the underlying composition dependence of the order parameters. Maier-Saupe theory predicts the species with the lower pure-component T_{NI} always has the lower order parameter in a mixture. In the present system that would imply that the order parameter of 350HSiCB4 (T_{NI} = 63 °C) would always be greater than that of 5CB (T_{NI} = 35 °C). This is clearly not the case over the range of concentration in which we can measure the component order parameters (polymer concentrations up to 10 wt %). ^{2}H NMR data from these solutions are in clear opposition to the mixing rule based on the Maier-Saupe model, showing that the order parameter of 350HSiCB4 is less than that of 5CB despite its higher clearing point in the bulk. The Brochard model gives phase diagrams with elevated T_{NI} at intermediate ϕ by allowing the nematic potential between the two species, U_{AB}, to be greater than those for the individual species, $c = U_{AB}/(U_{AA}U_{BB})^{1/2} > 1$. In this case, the Maier-Saupe mixing rule predicts that

addition of the high T_{NI} species to the low T_{NI} species will increase the order parameter of the latter. In the present system that would imply that the order parameter of 5CB would increase upon addition of polymer, which is clearly not the case: both ^{2}H NMR and refractive index data show that S of 5CB decreases as polymer concentration increases from 0 to 10 wt %.

Maier-Saupe theory assumes that mesogens interact with one another entirely through van der Waals forces, and the theory's failure to describe the measured component order parameters suggests that additional thermodynamic interactions are of importance in mixtures of 350HSiCB4 and 5CB. Indeed, it has been suggested by other authors that backbone flexibility and steric effects may have a strong influence on SGLCP/LC phase behavior.[4, 7, 8, 14] Compared to the systems modeled by Chiu and Kyu, et al.[11-13] using Brochard's theory, 350HSiCB4/5CB is similar with respect the structural details of the polymer and solvent. Fits were performed to experimental data from systems employing both phenyl benzoate-based and cyanobiphenyl-based mesogens, some with polymer mesogens that are chemically similar to the solvent[4, 5, 13] and some where the mesogens are mismatched.[11, 16] They furthermore modeled SGLCPs having different types of backbones, including polysiloxane[4, 5, 16], polyacrylate[11], and poly(ethylene glycol)[13] derivatives. Their fitting to the Brochard model is equally successful for this diverse group of SGLCP/LC systems, indicating that its failure to describe data from 350HSiCB4/5CB is not simply a consequence of the species' chemical structures. The one noteworthy difference between the present SGLCP and prior systems is its extremely high molecular weight. Data fit to the Brochard model previously were from polymers having molecular weights of approximately 50 kg/mol (degree of polymerization of approximately 100), but 350HSiCB4 is almost ten times as large. The influence of polymer length in the Brochard model enters via the Flory-Huggins interaction. Therefore, increasing the chain length can open biphasic windows in the phase diagram (or increase their width). However, Brochard's model has no coupling between the polymer backbone and the nematic order of the pendant mesogens, so changing SGLCP length has no effect on the order parameter of either species.

There must be an important thermodynamic contribution from the polymer that is unaccounted for in Brochard's model, which assumes the mesogens of an SGLCP are completely decoupled from the backbone. The coupling of the polymer backbone's conformational entropy to the nematic orientation field is neglected by Brochard's theory, but likely makes an important contribution to the thermodynamics of mixtures of 350HSiCB4 and 5CB. Indeed, such an effect could also play a major role in the thermodynamics of previously studied SGLCP/LC systems. In the bulk polymer, the tendency of the mesogenic side groups to align with one another competes with the polymer's conformational entropy and the system is highly frustrated (Figure 4.10d). It appears that at compositions intermediate between bulk polymer and dilute solution the solvent serves to increase the polymer's configurational freedom, allowing it to relax some of the frustration present in the melt. The strong, non-monotonic dependence of $|\Delta H|$ and onset T on polymer concentration, especially at compositions near bulk polymer, suggests the effect is related to the two components' relative proportions. We envision that the peak in $|\Delta H|$ arises from maximizing the mesogens' orientational order while minimizing the polymer's perturbation from a random-walk conformation (Figure 4.10c). If we consider the opposite extreme, starting from pure LC and adding SGLCP to it, we introduce a population of mesogens that are constrained by attachment to the polymer. In this regime we envision that the compromise between LC orientation and conformational entropy causes the order parameters of both polymer and solvent drop as a result of the orientational frustration between the two (Figure 4.10b).

It might be possible to rigorously account for the coupling between polymer entropy and LC order by including effects of chain flexibility, similar to the theory of ten Bosch, Maissa, and Sixou for main-chain polymers.[34] In the absence of such a theory, the coupling can be empirically accounted for by introducing concentration dependence to the polymer-solvent nematic interaction parameter, U_{AB}. By doing so, the concentration dependence of the nematic-isotropic transition temperatures can be correctly captured, but the relative magnitudes of the component order parameters still cannot. The theoretical T_{NI}'s of 350HSiCB4/5CB mixtures were calculated from Equation 4.2 at fixed values of c between 0.8 and 1.2 (Figure 4.11a). The c values necessary to describe the data were used

to generate a continuous function $c(\phi_B)$ using a B-spline (Figure 4.11b). The empirical $c(\phi_B)$ was then used to calculate a theoretical diagram using Brochard's model with the Flory interaction parameter arbitrarily set to $\chi = 350 / T$ (Figure 4.11c). The theoretical phase diagram resembles that inferred from the DSC data (Figure 4.9a); however, there is no physical basis for choosing a concentration dependence of U_{AB}. This exercise does serve to emphasize the idea that the interplay between polymer entropy and LC orientation depends strongly on the relative proportions of the two components and plays an important role in the system's thermodynamics that is not accounted for in Brochard's model.

4.5 Conclusions

4.5.1 Conclusions Based on the Present Work

The delicate thermodynamic balance between liquid crystalline order and polymer conformational entropy serves to stabilize the nematic phase in mixtures of 350HSiCB4 and 5CB. In dilute solutions, the tradeoff between the two causes the order parameter of the polymer side-groups to be less than that of the solvent. As concentration is increased, the orientational frustration between the two decreases the solvent order parameter as well. When the polymer concentration is increased to the range of 70 to 85 wt.-%, the minority fraction of small-molecule solvent affords the SGLCP freedom to optimize LC order subject ot the connectivity between the polymer backbone and its pendant side-groups, raising the nematic-isotropic transition temperature almost 20 °C above that of the bulk polymer and almost 45 °C higher than that of the LC solvent alone. Thus, the SGLCP must also provide a favorable host for 5CB.

The results presented here are in stark contrast to the body of literature on solutions of SGLCPs in nematic solvent. Stabilization of the nematic phase is rarely[16] observed in these systems and the LC orientation is usually concluded to be decoupled from the conformational entropy of an SGLCP. Our results suggest an avenue for future theoretical work that accounts for the interplay between the polymer's conformational entropy and liquid crystalline order in a regime intermediate between strong coupling (e.g. main-chain

polymers, as considered by ten Bosch et al.[38]) and complete decoupling (Brochard's theory for side-chain polymers).

4.5.2 Suggestions for Future Experiments

^{2}H NMR spectroscopy and refractive index measurements are limited to the dilute regime because of the difficulty in aligning the samples. However, these results beg the question: what is the relative orientation order of the polymer and solvent at higher concentration? Small-angle neutron scattering experiments on selectively labeled polymer solutions might reveal a strong concentration dependence of the polymer's conformational anisotropy and provide evidence of orientational coupling, or wide-angle x-ray scattering experiments could be used to measure the nematic order parameter in the concentrated regime. It would, furthermore, be of interest to study the molecular weight dependence of the polymer's phase behavior, perhaps using smaller polymers to compare with previous studies more directly.

4.6 Tables

Table 4.1 Molecular weight, conversion, and polydispersity of the side-group liquid crystal homopolymers. Details of characterization may be found in Appendix A.

Name	M_n (kg/mol)	Mole Fraction 1,2 PB	Mole Fraction 1,4 PB	Mole Fraction LC	PDI[a]
350HSiCB4	347	0	0.11	0.89	1.27
$d_2$350HSiCB4	348	0	0.11	0.89	1.27
490HSiCB4	489	0.01	0.03	0.96	1.48

[a]PDI = Polydispersity Index (M_w/M_n)

4.7 Figures
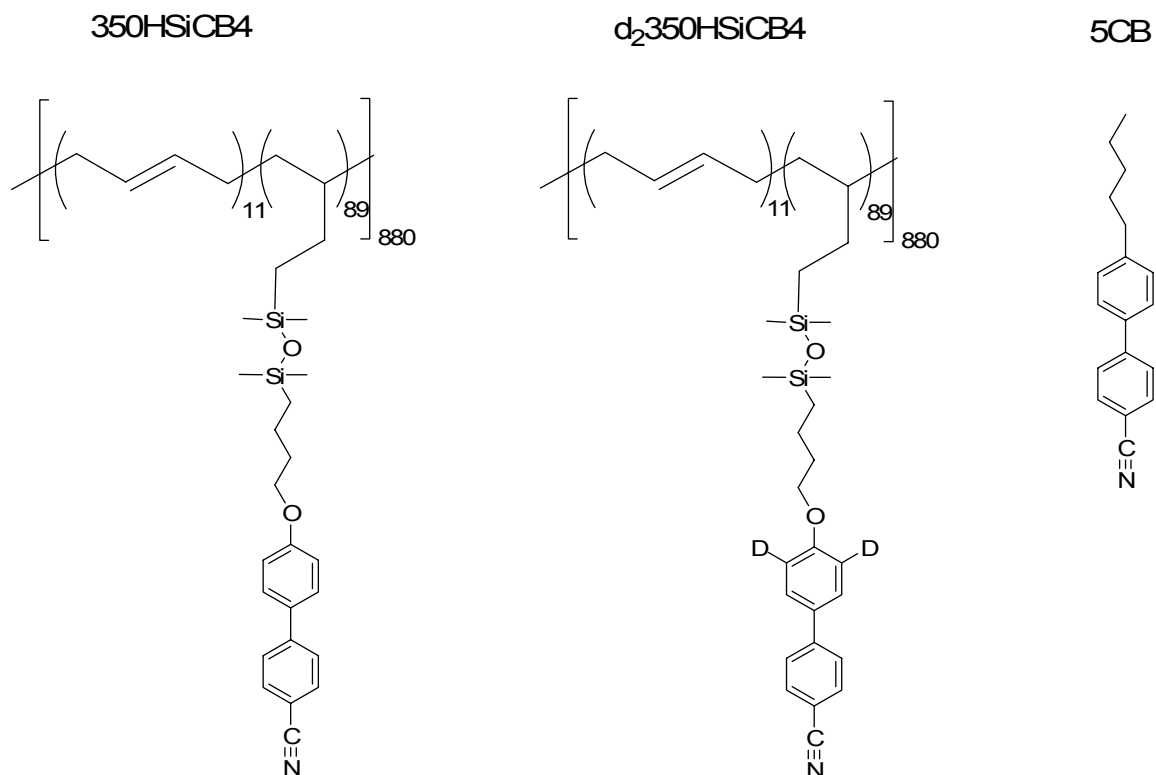
Figure 4.1 Chemical structures of the end-on side-group liquid crystal polymers (350HSiCB4 and d$_2$350HSiCB4) and the nematic liquid crystal solvent (5CB). The polymer's name is derived from its molecular weight (350 kg/mol), the letter "H" to indicate a homopolymer, and "SiCB4" to indicate end-on mesogens. In addition to monomers having an attached mesogen, the polymer also contains some residual 1,2- and 1,4-butadiene monomers. The polymers' properties are summarized in Table 4.1. Full details of polymer characterization are given in Appendix A.
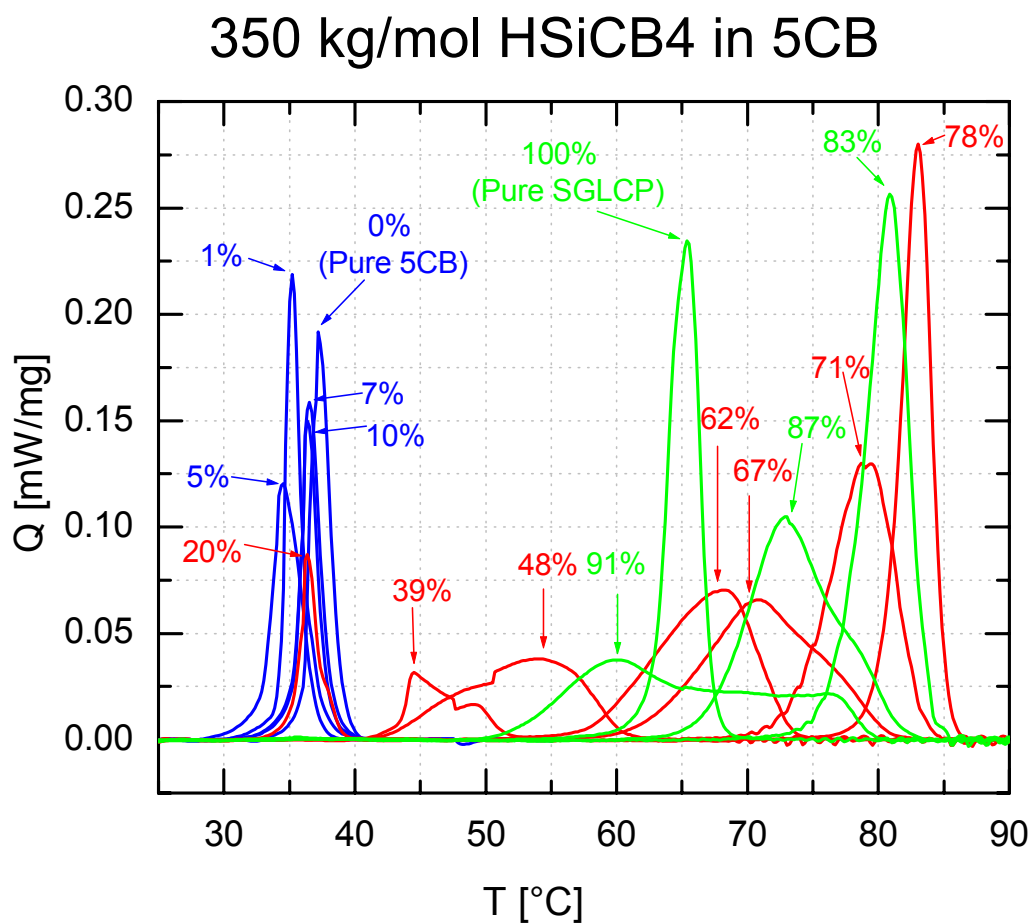
Figure 4.2 DSC temperature scans from mixtures of 350HSiCB4 and 5CB in proportions ranging from 0 to 100 wt % polymer obtained on heating. The peak position changes very little as concentration is increased from 0 to 20 wt % polymer (blue curves), then shifts to higher temperature as concentration is increased from 39 to 78 wt % polymer (red curves). Above 78 wt % polymer the peak position shifts to lower *T* with increasing concentration (green curves). Baselines were subtracted from the DSC scans as described in the text; in some cases the procedure produced a small discontinuity in the baseline, leading to the discontinuities evident in some of the baseline subtracted curves.
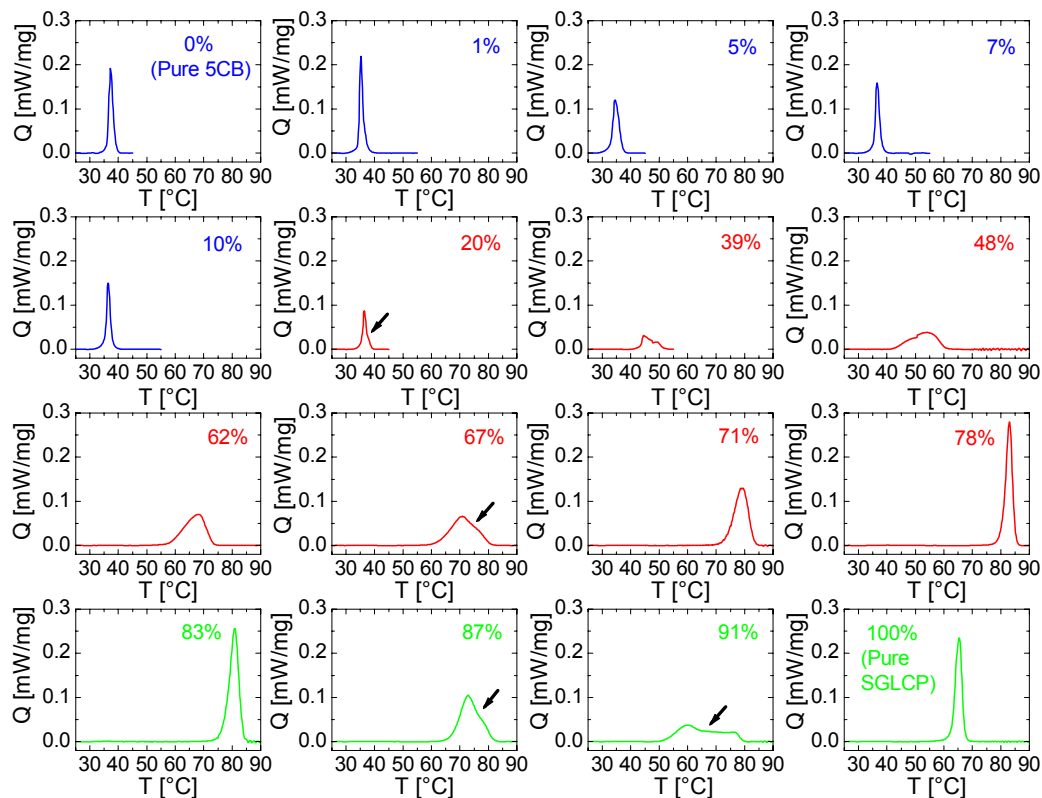
Figure 4.3 DSC temperature scans from Figure 4.2 plotted individually for clarity. The peak position changes very little as concentration is increased from 0 to 20 wt % polymer (blue curves), then shifts to higher temperature as concentration is increased from 39 to 78 wt % polymer (red curves). Above 78 wt % polymer the peak position shifts to lower T with increasing concentration (green curves). Arrows are used to indicate shoulders in the phase transition endotherms. Baselines were subtracted from the DSC scans by fitting to second degree piecewise polynomials and data were normalized by the sample weight to give normalized, subtracted heat flow, Q.

350HSiCB4 in 5CB

(a)

(b)
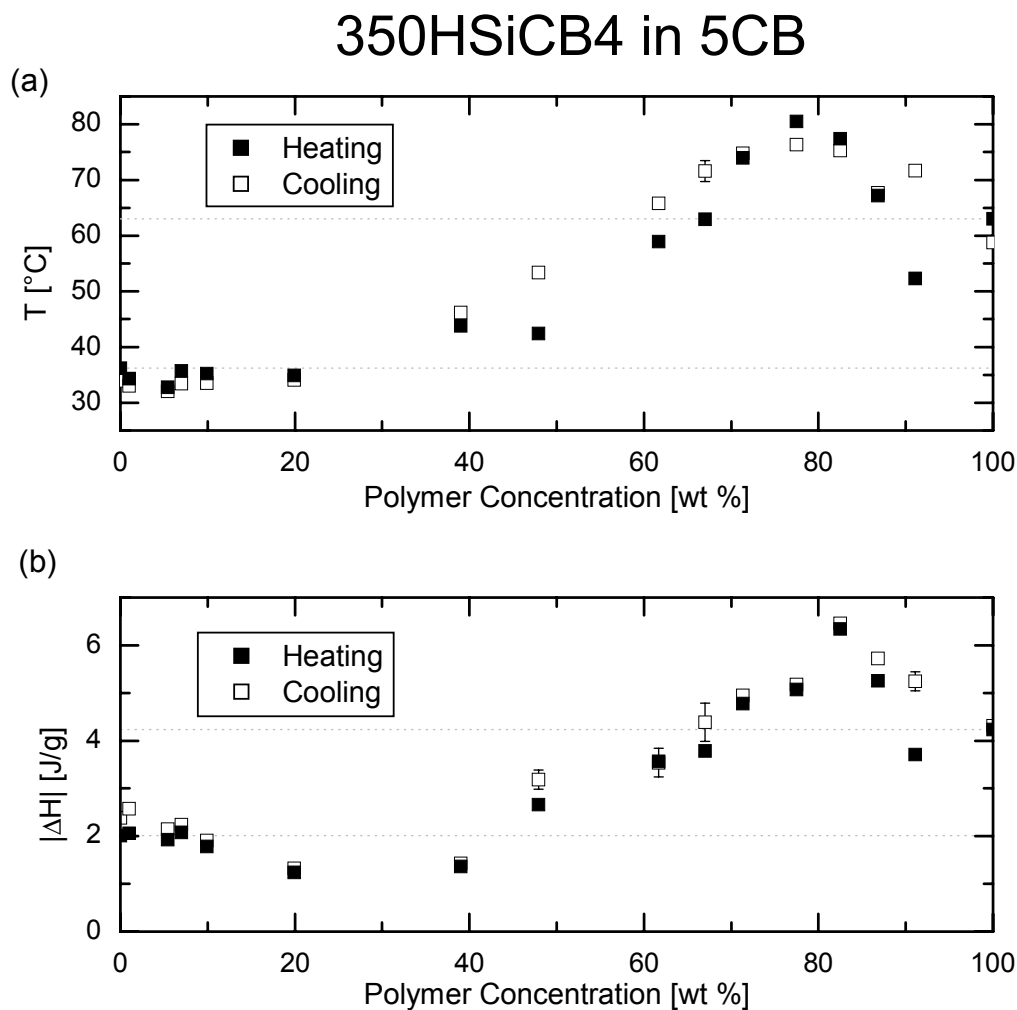
Figure 4.4 Latent heat ($|\Delta H|$) and onset temperature (T) of the nematic/isotropic phase transition measured from DSC scans on heating and cooling in mixtures of 350HSiCB4 with 5CB as a function of polymer concentration. Data points are the average of six consecutive temperature scans and error bars indicate the standard deviation. Dotted lines indicate the onset temperatures for pure 5CB and SGLCP.
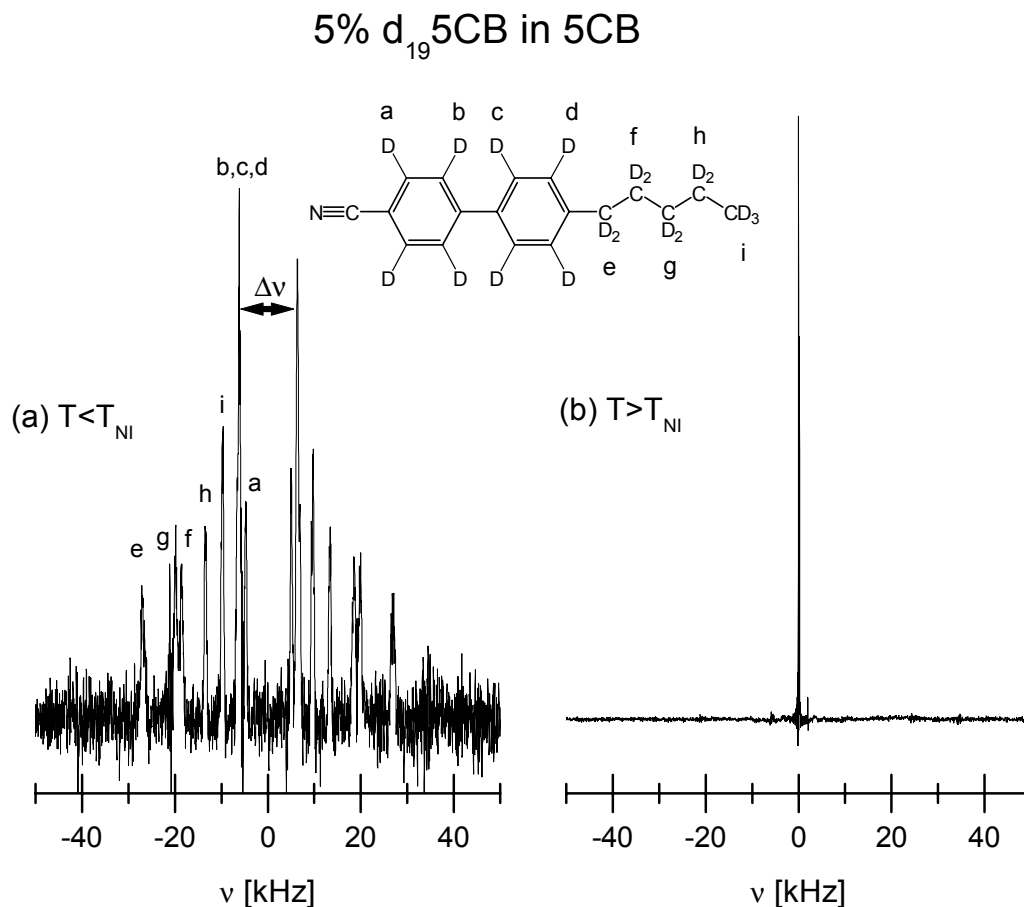
5% d$_{19}$5CB in 5CB

Figure 4.5 Representative ^{2}H NMR spectrum of 5 wt % d$_{19}$5CB in 5CB taken at (a) $T = T_{NI} - 8$ °C and (b) $T = T_{NI} + 2$ °C (b)   (a) Orienational order in the nematic phase ($T < T_{NI}$) gives rise to a symmetric spectrum where the quadrupolar splitting, Δv, for each set of equivalent deuterons depends on the microscopic order parameter and the angle between the director and the magnetic field.   Peak assignments have been made according to Auger et al.[30]   (b) In the isotropic phase ($T > T_{NI}$) the quadrupolar interactions are averaged to yield a single peak centered at $v = 0$.
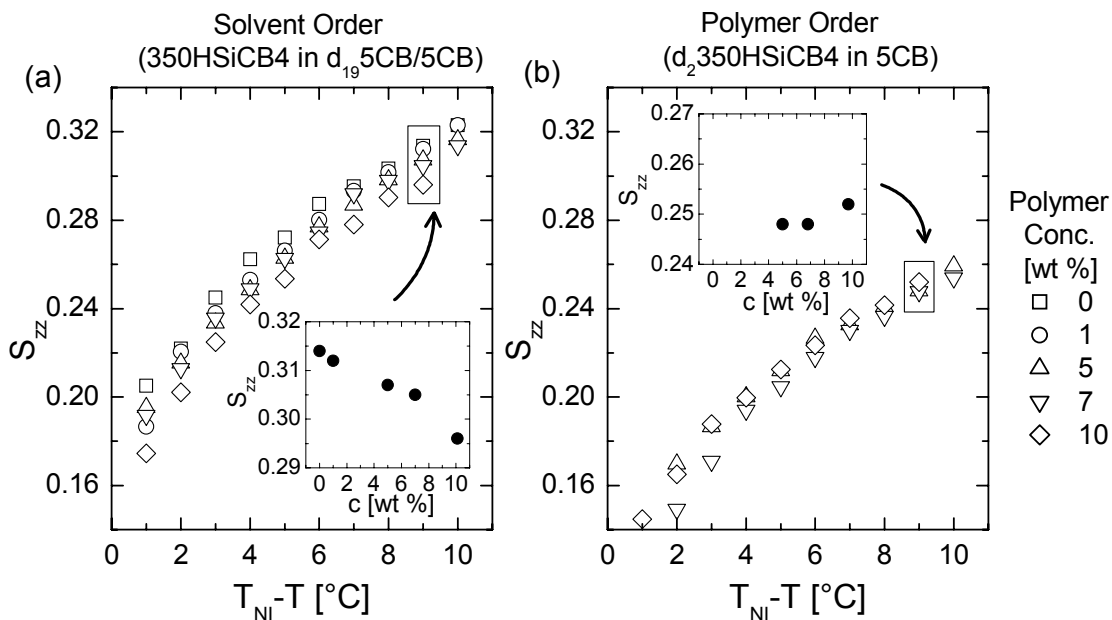
Figure 4.6 Microscopic order parameters, S_{zz}, measured from quadrupolar splittings, $\Delta\nu$, of (a) aromatic deuterium atoms located *para-* to the alkyl chain in $d_{19}5CB$ and (b) aromatic deuterium atoms located *para-* to the oxygen atom in $d_2350HSiCB4$ as a function of reduced temperature, $T_{NI} - T$, containing various polymer concentrations, c, (legend to the right applies to both graphs). The dependence of $\Delta\nu$ on polymer concentration (*c*) at $T = T_{NI} - 9\ °C$ is expanded in the inset plot.
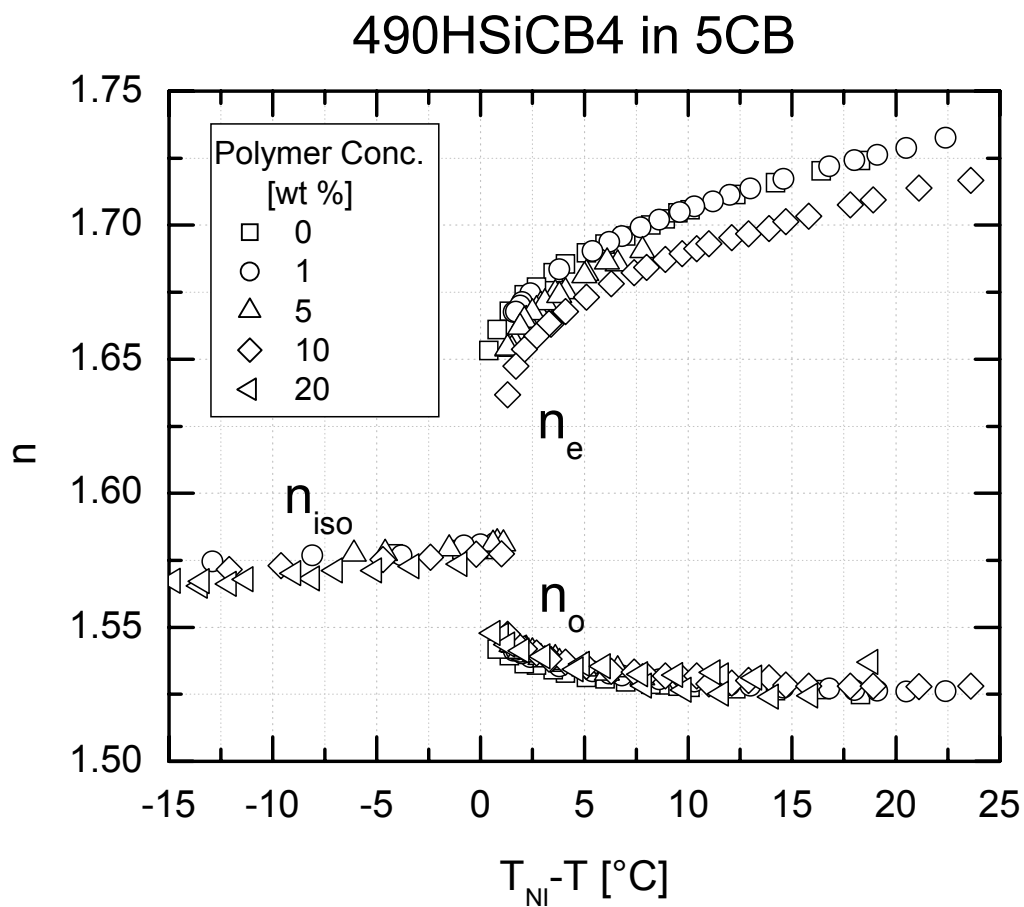
Figure 4.7 Temperature dependence of the ordinary, n_o, and extraordinary, n_e, refractive indices of pure 5CB and solutions of 490HSiCB4 in 5CB in the nematic phase and in the isotropic phase, n_{iso}.
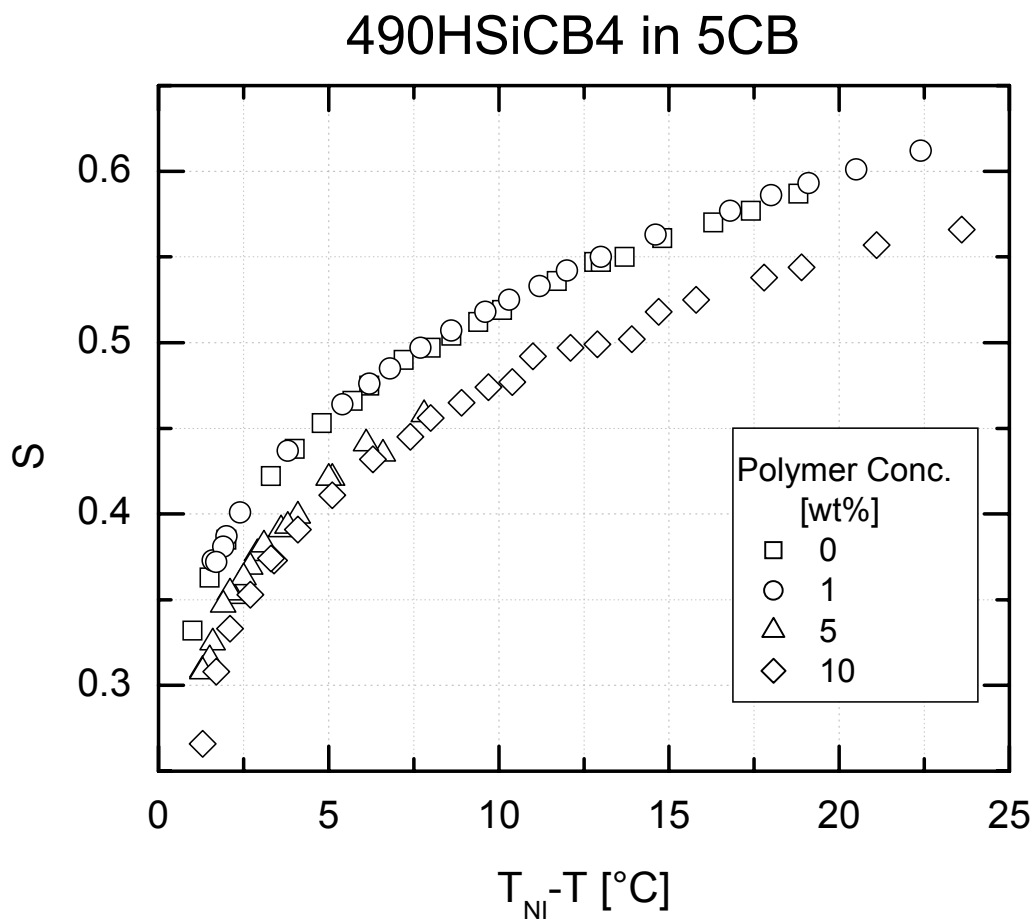
Figure 4.8 Temperature dependence of the order parameter (*S*) of 5CB, and solutions of 490HSiCB4 in 5CB, determined from refractive index measurements. In performing the Haller analysis[32], the density and molar mass for polymer solutions were assumed equal to those of 5CB[31] ($\rho = 1$ g/cm^3, $M = 249$ g/mol).
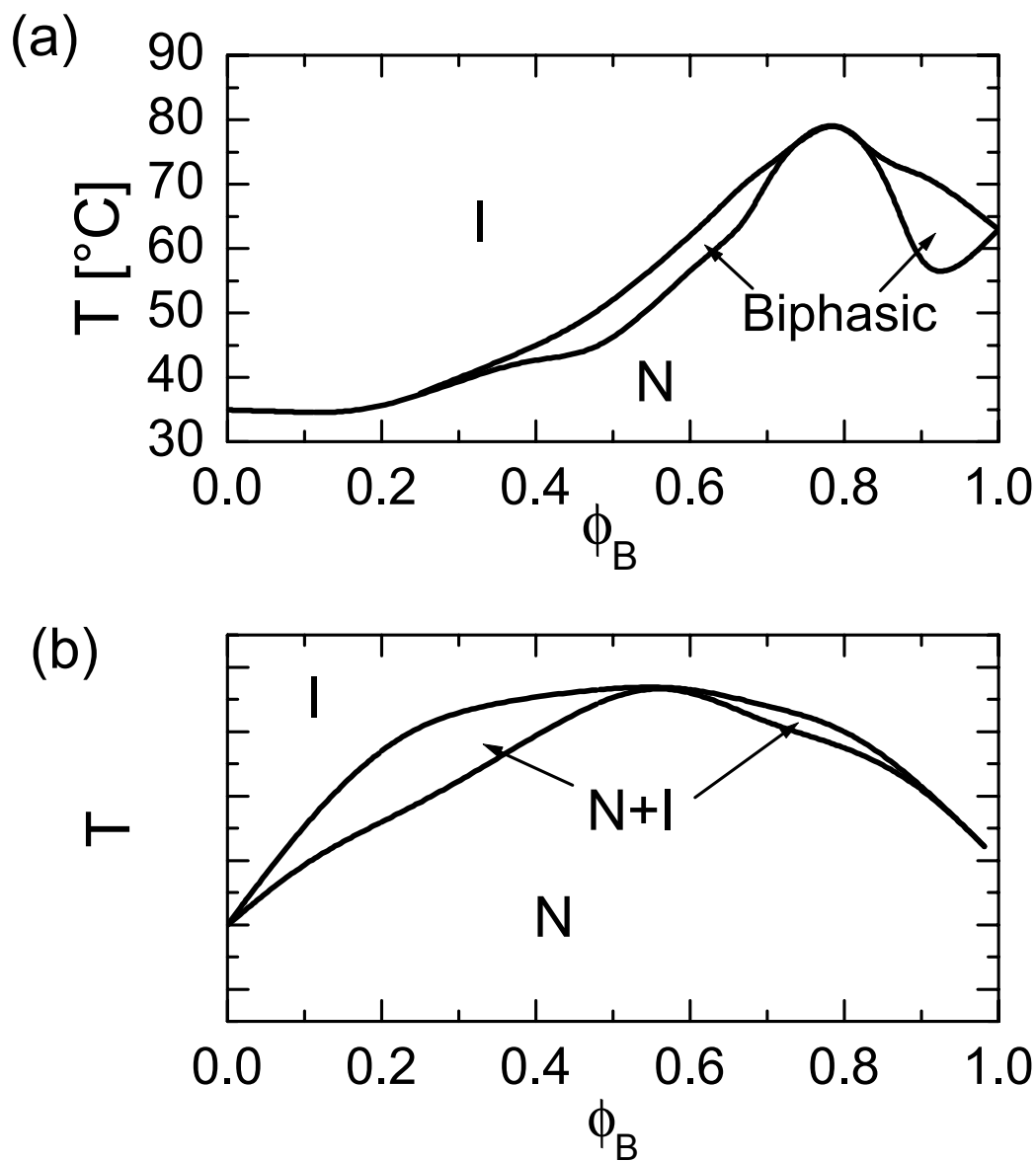
(a)

(b)

Figure 4.9 (a) Schematic representation of a plausible phase diagram deduced from DSC data. The letter "*N*" represents a single nematic phase and the letter "*I*" represents a single isotropic phase. (b) Schematic representation of a phase diagram calculated by Chiu and Kyu[12] using Brochard's model[15] for an SGLCP polymer and a small-molecule LC with strong nematic interactions between the two ($c = U_{AB}/(U_{AA}U_{BB})^{1/2} = 1.2$).
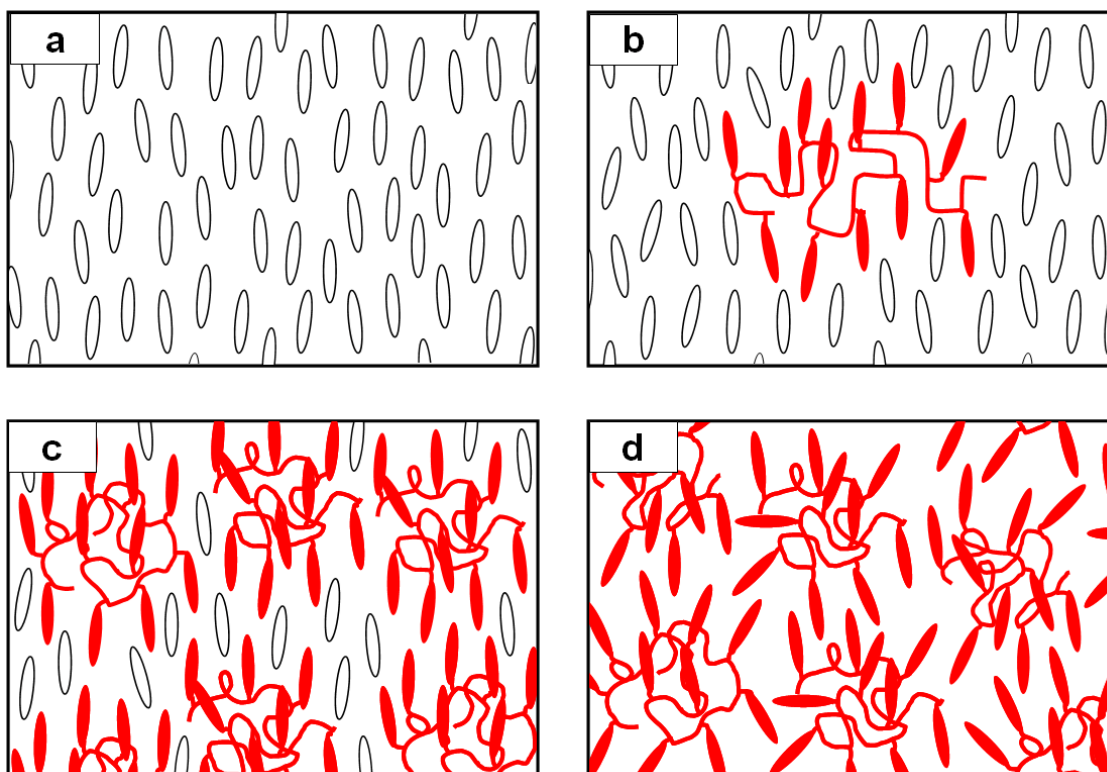
Figure 4.10 Schematic representation of mixtures of 350HSiCB4 with 5CB at various concentrations. Mesogens are represented by white (5CB) and red (350HSiCB4) ellipses. (a) 5CB without any dissolved polymer. (b) A dilute solution of polymer in 5CB. The polymer adopts an anisotropic conformation because of its coupling to the solvent's director field. (c) Polymer with a small amount of 5CB, corresponding to the stabilized nematic phase at approximately 80 wt.-% 350HSiCB4. The solvent serves to increase the polymer's configurational freedom, allowing it to relax some of the frustration present in the melt. (d) Bulk polymer without any small-molecule solvent. The polymer's mesogens are strongly coupled to the backbone conformation.
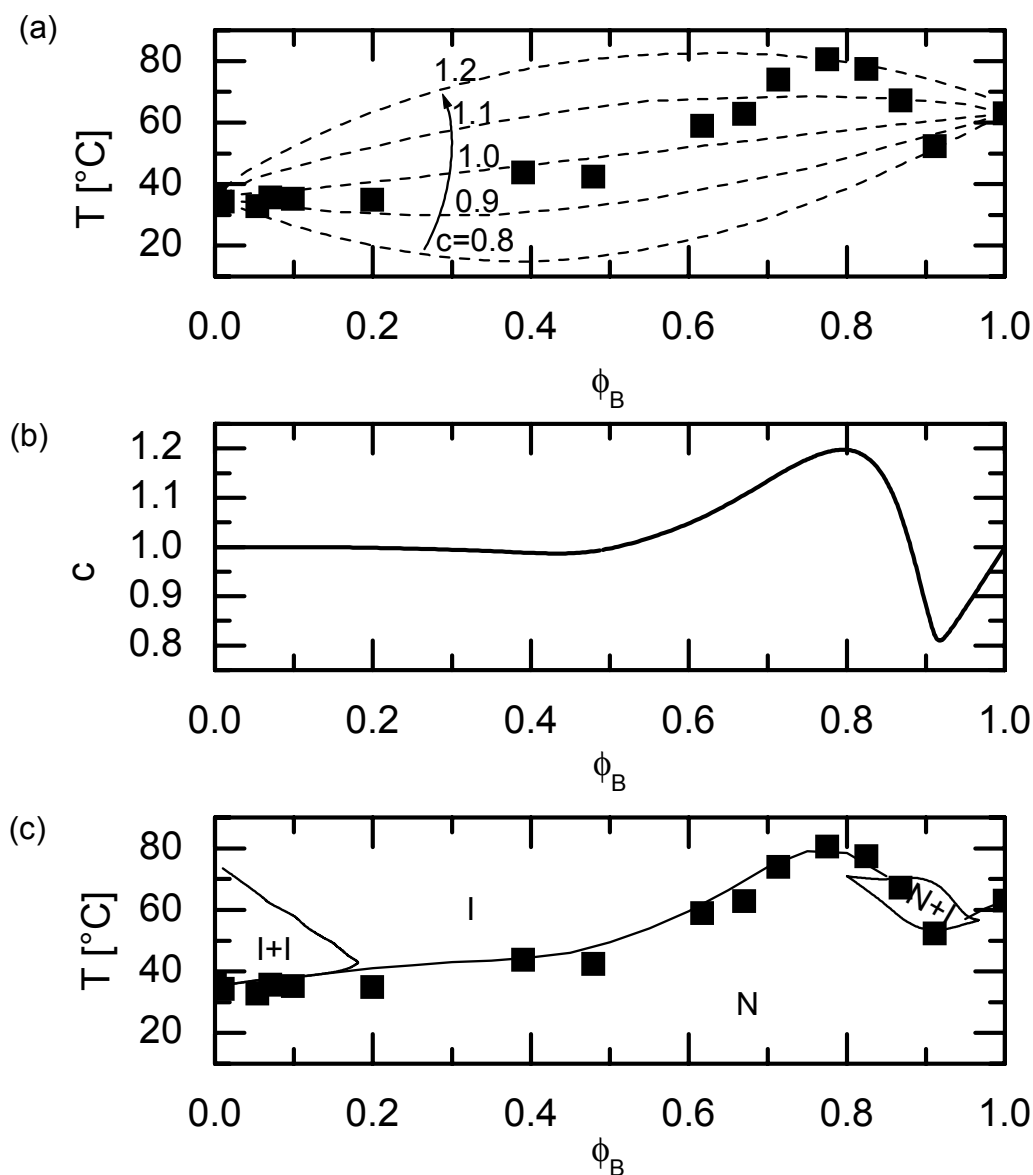
Figure 4.11 (a) Nematic-isotropic transition temperatures predicted by Maier-Saupe theory using values of $c = U_{AB} / (U_{AA}U_{BB})^{1/2}$ between 0.8 and 1.2 (dotted lines) together with phase transition onset temperatures of 350HSiCB4/5CB measured by DSC on heating (solid squares). (b) The imposed concentration-dependence of c used to generate the phase diagram in (c). (c) Phase boundaries (solid lines) predicted by Brochard's model using a concentration-dependent polymer-solvent nematic interaction parameter, U_{AB}, together with phase transition onset temperatures of 350HSiCB4/5CB measured by DSC on heating (solid squares). "N" and "I" indicate single nematic and isotropic phases, respectively. "$I+I$" indicates two coexisting isotropic phases and "$N+I$" indicates coexistence of a nematic and an isotropic phase. The Flory interaction parameter was arbitrarily set to $\chi = 350 / T$. In (a), (b), and (c), ϕ_B is the volume fraction of polymer.

4.8 References

[1]   Benmouna, F.; Daoudi, A.; Roussel, F.; Buisine, J.-M.; Coqueret, X.; Maschke, U. Equilibrium Phase Diagram of Polystyrene and 8CB. *J. Polym. Sci., Part B: Polym. Phys.* **1999**, *37*, 1841-1848.

[2]   Gogibus, N.; Maschke, U.; Benmouna, F.; Ewen, B.; Coqueret, X.; Benmouna, M. Phase Diagrams of Poly(dimethylsiloxane) and 5CB Blends. *J. Polym. Sci., Part B: Polym. Phys.* **2001**, *39*, 581-588.

[3]   Kihara, H.; Kishi, R.; Miura, T.; Kato, T.; Ichijo, H. Phase behavior of liquid-crystalline copolymer/ liquid crystal blends. *Polymer* **2001**, *42*, 1177-1182.

[4]   Casagrande, C.; Veyssie, M.; Finkelmann, H. Phase separations in the mixtures of a mesomorphic polymer with a low molecular mass liquid crystal. *J. Physique* **1982**, *43*, L671 - L675.

[5]   Finkelmann, H.; Kock, H.-J.; Rehage, G. Phase Studies of Liquid Crystalline Side Chain Polymers Mixed with Low Molar Mass Liquid Crystals of Similar Structure. *Mol. Cryst. Liq. Cryst.* **1982**, *89*, 23-36.

[6]   Ringsdorf, H.; Schmidt, H.-W.; Schneller, A. Miscibility Studies of Polymeric and Low Molecular Weight Liquid Crystals and Their Behaviour in an Electric Field. *Makromol. Chem., Rapid Commun.* **1982**, *3*, 745-751.

[7]   Benthack-Thoms, H.; Finkelmann, H. Phase separations in binary mixtures of nematic liquid crystal side chain polymers and low-molar-mass liquid crystals, 1 Influence of the chemical constitution of the low-molar-mass component. *Makromol. Chem.* **1985**, *186*, 1895-1903.

[8]   Gilli, J. M.; C., F.; Sixou, P.; Robert, P.; Villenave, J. J.; Fontanille, M. New Thermotropic Polymers with Flexible Backbone and Mesogenic Side Chains: Blends with Small Molecule Liquid Crystals. *Mol. Cryst. Liq. Cryst.* **1989**, *167*, 73-87.

[9]   Sigaud, G.; Achard, M. F.; Hardouin, F.; Coulon, C.; Richard, H.; Mauzac, M. Flory's Parameters in Solutions of Liquid Crystalline Side-Chain Polymers in Low Molecular Weight Liquid Crystals. *Macromolecules* **1990**, *23*, 5020-5024.

[10]   Sigaud, G.; Achard, M. F.; Hardouin, F.; Mauzac, M.; Richard, H.; Gasparoux, H. Relationships between Molecular Structure and Immiscibility of Liquid Crystalline Side-Chain Polymers in Low Molecular Weight Nematic Solvents. *Macromolecules* **1987**, *20*, 578-585.

[11]   Chang, M. C.; Chiu, H. W.; Wang, X. Y.; Kyu, T.; Leroux, N.; Campbell, S.; Chien, L. C. Phase transitions in mixtures of a side-on-side chain liquid crystalline polymer and low molar mass nematic liquid crystals. *Liq. Cryst.* **1998**, *25*, 733-744.

[12]   Chiu, H.-W.; Kyu, T. Equilibrium phase behavior of nematic mixtures. *J. Chem. Phys.* **1995**, *103*, 7471-7481.

[13]   Chiu, H.-W.; Zhou, Z. L.; Kyu, T.; Cada, L. G.; Chien, L.-C. Phase Diagrams and Phase Separation Dynamics in Mixtures of Side-Chain Liquid Crystalline Polymers and Low Molar Mass Liquid Crystals. *Macromolecules* **1996**, *29*, 1051-1058.

[14]   Attard, G. S.; Karasz, F. E. Phase studies of blends of polystyrene-based liquid-crystalline side-chain polymers with low-molar-mass mesogens. *Makromol. Chem., Rapid Commun.* **1990**, *11*, 145-150.

[15] Brochard, F.; Jouffroy, J.; Levinson, P. Phase diagrams of mesomorphic mixtures. *J. Physique* **1984**, *45*, 1125-1136.

[16] Hwang, J. C.; Kikuchi, K.; Kajiyama, T. Aggregation states and electro-optical properties of the induced smectic phase by mixing a nematic liquid crystalline polymer and a low molecular weight liquid crystal. *Polymer* **1992**, *33*, 1822-1825.

[17] Ratto, J. A.; Volino, F.; Blumstein, R. B. Phase Behavior and Order in Mixtures of Main-Chain Nematic Polyesters with Small Molecules: A Combined Proton and Deuterium NMR Study. *Macromolecules* **1991**, *24*, 2862-2867.

[18] Volino, F.; Gauthier, M. M.; Giroud-Godquin, A. M. NMR Study of Dilute Solutions of Main-Chain Nematic Polyesters in *p*-Azoxyanisole. *Macromolecules* **1985**, *18*, 2620-2623.

[19] de Gennes, P.-G. *The Physics of Liquid Crystals*, 2nd ed; Clarendon Press: Oxford, 1993.

[20] Haller, I.; Huggins, H. A.; Freiser, M. J. Measurement of Indices of Refraction of Nematic Liquids. *Mol. Cryst. Liq. Cryst.* **1972**, *16*, 53-59.

[21] Kempe, M. D.; Kornfield, J. A. Shear alignment behavior of nematic solutions induced by ultralong side-group liquid crystal polymers. *Phys. Rev. Lett.* **2003**, *90*, 115501.

[22] Mansare, T.; Decressain, R.; Gors, C.; Dolganov, V. K. Phase Transformations and Dynamics of 4-Cyano-4'-Pentylbiphenyl (5CB) by Nuclear Magnetic Resonance, Analysis Differential Scanning Calorimetry, and Wideangle X-Ray Diffraction Analysis. *Mol. Cryst. Liq. Cryst.* **2002**, *382*, 97-111.

[23] Van Roie, B.; Leys, J.; Denolf, K.; Glorieux, C.; Pitsi, G.; Thoen, J. Weakly first-order character of the nematic-isotropic phase transition in liquid crystals. *Phys. Rev. E* **2005**, *72*, 041702.

[24] Finkelmann, H.; Kock, H.-J.; Rehage, G. Investigations on liquid crystalline polysiloxanes 3. Liquid crystalline elastomers -- a new type of liquid crystalline material. *Makromol. Chem., Rapid Commun.* **1981**, *2*, 317-322.

[25] Dong, R. R. *Nuclear Magnetic Resonance of Liquid Crystals*, 2nd ed; Partially Ordered Systems, ed. L. Lam; D. Langevin; Springer: New York, 1997.

[26] Tabayashi, K.; Akasaka, K. Natural Abundance ^{2}H NMR for Liquid Crystal Studies. Application to 4'-(Hexyloxy)-4-cyanobiphenyl. *J. Phys. Chem. B* **1997**, *101*, 5108-5111.

[27] Emsley, J. W.; Luckhurst, G. R.; Stockley, C. P. The deuterium and proton-{deuterium} N.M.R. spectra of the partially deuterated nematic liquid crystal 4-n-penyl-4'-cyanobiphenyl. *Mol. Phys.* **1981**, *44*, 565-580.

[28] Emsley, J. W.; Foord, E. K.; Gandy, P. J. F.; Turner, D. L. Assignment of the quadrupolar splittings in fully deuteriated alkyl chains of liquid crystalline compounds The case of 4-n-hexyloxy-4'-cyanobiphenyl. *Liq. Cryst.* **1994**, *17*, 303-309.

[29] Luckhurst, G. R. Pretransitional Behaviour in Liquid Crystals. *J. Chem. Soc., Faraday Trans. 2* **1988**, *84*, 961-986.

[30] Auger, C.; Lesage, A.; Caldarelli, S.; Hodgkinson, P.; Emsley, L. Assignment and Measurement of Deuterium Quadrupolar Couplings in Liquid Crystals by

Deuterium-Carbon NMR Correlation Spectroscopy. *J. Phys. Chem. B* **1998**, *102*, 3718-3723.

[31]   Karat, P. P.; Madhusudana, N. V. Elastic and Optical Properties of Some 4'-n-Alkyl-4-Cyanobiphenyls. *Mol. Cryst. Liq. Cryst.* **1976**, *36*, 51-64.

[32]   Haller, I.; Huggins, H. A.; Lilienthal, H. R.; McGuire, T. R. Order-Related Properties of Some Nematic Liquids. *J. Phys. Chem.* **1973**, *77*, 950-954.

[33]   Woo, I.-C.; Wu, S.-T. *Optics and Nonlinear Optics of Liquid Crystals*, World Scientific: River Edge, NJ, 1993.

[34]   ten Bosch, A.; Maissa, P.; Sixou, P. Molecular model for nematic polymer in liquid crystal solvents. *J. Chem. Phys.* **1983**, *79*, 3462-3466.